

<sup>2</sup>Acibadem Altunizade Hospital, Department of Radiotherapy, Istanbul, Turkey

### Purpose or Objective

MVCT imaging is done for pretreatment patient position verification in Tomotherapy system. MVCT images are registered to treatment planning CT images and translational setup errors are corrected via couch shifts. Additionally rotational setup errors in longitudinal axis (Roll) are compensated automatically changing start position of the gantry angle. The purpose of this study is to dosimetrically evaluate the reliability of roll correction of the Tomotherapy system.

### Material and Methods

Target and avoidance structures (AS) were delineated on the Cheese phantom CT images in VoLO treatment planning system (Version 5.1) and three different helical treatment plans were made. First plan was created only to cover target but not blocked AS (unblocked, UB). Directional Blocked (DB) option was used in second plan and complete blocked (CB) option was chosen in third plan to protect AS. Cheese phantom was positioned on the treatment couch. EBT3 film was placed between slabs to evaluate two dimensional dose distribution and 0.125 cc ion chamber (IC) was inserted to the 0.5 cm depth hole to measure point dose. The roll angle of the phantom was adjusted at 0° using digital leveling device (LD) and three of the plans were irradiated. Films were changed and IC measurements were also noted for each plan. These 0° measurements were taken as reference. Cheese phantom was rotated 1°, 3°, 5° and 10° in clockwise (CW) and counter clockwise (CCW) directions using LD. After acquire MVCT images of the phantom, these roll angles were entered as roll setup correction angle to the system and all plans were irradiated for each angle. Film and IC measurements were repeated for each angle and each plans. Exposed films were compared with reference films using gamma analysis method in PTW verisoft software (version 7.0). The passing criteria in gamma analysis was 3mm and %3 for distance to agreement and dose differences respectively. In addition IC measurements were compared with reference point doses.

### Results

For gamma value <1, max-min values were 99.8-97.2% for UB plans, 98.5-97.2% for DB plans and 99.6-97.9% for CB plans. The min value was measured for 1° roll error in CCW direction for all three plans. Although the min gamma values were found in 1° CCW direction, gamma values were found in the limits for all plans, all roll angles and all directions. When IC measurements were compared, the differences were found < 1.5% for UB and DB plans and < 1% for CB plans.

### Conclusion

Roll setup corrections were successfully done by Tomotherapy system independently of plan complexity, the size of the rotation angle and the direction of the rotation.

### EP-1810 Assessing the dose significance of unplanned rectal filling in pelvic MR Guided Radiotherapy

J. Shortall<sup>1</sup>, E. Vasquez Osorio<sup>1</sup>, M. Van Herk<sup>2</sup>

<sup>1</sup>The University of Manchester, Division of Cancer Sciences, Manchester, United Kingdom

<sup>2</sup>The University of Manchester- The Christie NHS Foundation Trust, Division of Cancer Sciences, Manchester, United Kingdom

### Purpose or Objective

Propositions that opposing beams can be used to compensate for Electron Return Effect (ERE) during MR guided radiotherapy may not always be achievable in pelvic patients where rectal or intestine walls lie in the path of a single radiation beam. This work evaluates the dosimetric effects to the rectal wall due to ERE,

comparing unplanned gaseous and solid filling during pelvic MR guided therapy.

### Material and Methods

Monaco 5.19.02 (Elekta) was used to produce Monte Carlo simulations of a single radiation beam under the influence of a 1.5T transverse magnetic field. Contours representing a rectal wall containing solid or gaseous filling were simulated. The wall thickness was adapted to accommodate transverse expansion assuming a constant cross sectional area of 3.6cm<sup>2</sup>.

Fig. 1A illustrates a simulated rectal structure transversely expanded due to filling. Note that the wall thickness around the filling becomes thinner as the expansion increases. Fig. 1B and C present simulated dose distributions through a cross section of the rectal wall containing solid or gaseous filling respectively.

DVHs calculated with in house software were used to assess the dosimetric effects of ERE due to unplanned gaseous filling compared to solid filling. To omit effects due to geometrical changes, comparisons were made only between equivalent solid and gaseous filling.

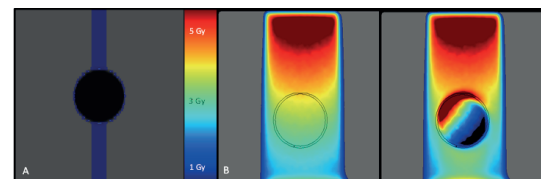


Figure 1 A) – The contoured rectal wall structure used to simulate rectal filling. This shows filling of approximately 100cm<sup>3</sup>, which is equivalent to a sphere of 6 cm diameter. Note that the wall becomes thinner depending on the transverse expansion. B) – The dose distribution of a single beam passing through the rectal wall expanded due to 100cm<sup>3</sup> solid filling. C) – Dose distribution of a single beam passing through the rectal wall expanded due to 100cm<sup>3</sup> gaseous filling.

### Results

No significant change to the mean rectal wall dose was found between solid and gaseous filling. Likely because the anterior overdosage due to ERE is counterbalanced by underdosage on the posterior aspect (Fig. 1C).

Differences are observed when comparing the maximum doses. Figure 2 shows the volume of rectal wall receiving an increased dose when unplanned gaseous filling occurs compared with solid filling. The maximum dose in the rectal wall increases by over 50% for large gaseous filling, compared to equivalent solid filling. Over 6cm<sup>3</sup> of the rectal wall is subject to a 20% dose increase when gaseous filling of over 100cm<sup>3</sup> occurs. It is indicated that ERE becomes more significant for larger gaseous filling, where a larger volume of rectal wall is exposed to a larger dose increase.

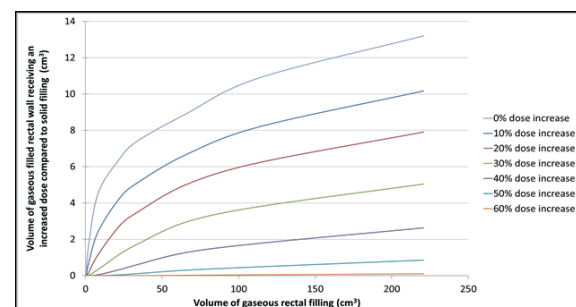


Figure 2 – The absolute volume of rectal wall that receives a relative dose increase due to ERE occurring during various volumes of gaseous filling, compared to the maximum dose received in the rectal wall during solid filling. Each coloured line represents a fixed percentage increase to the rectal wall.

### Conclusion

Although the mean dose is unaffected, unplanned gaseous filling subjects the rectal wall to sizeable hotspots where doses in the rectal wall are increased by over 50% compared to solid filling. Generally, this effect becomes more significant for larger gaseous volumes contained in a single beam. However, considering multiple beams is anticipated to reduce this effect.

This work can eventually be used to determine safety margins on dosimetrical constraints for intestinal OARs. Further work to assess different beam orientations and overlap in and beyond the rectal wall, particularly in nearby PTV areas, should be done. Note that the time that gaseous filling occurs for during treatment could have clinical implications on constraints. Dosimetrical effects due to anatomical changes arising from expansions of the rectal wall should also be incorporated.

**EP-1811 Dosimetric evaluation of a novel MC dose calculation algorithm for robotic radiosurgery with MLC**  
 S.C. Heidorn<sup>1</sup>, N. Kremer<sup>1</sup>, C. Fürweger<sup>1</sup>  
<sup>1</sup>European Cyberknife Center Munich, Medical physics, Munich, Germany

#### Purpose or Objective

Since clinical introduction of the first MLC to be mounted on a robotic SRS/SBRT platform in 2015, dose calculation with a Finite-Sized Pencil Beam (FSPB) algorithm has been the only available option. Due to limitations of this calculation technique, use of the MLC in a heterogeneous situation such as lung SBRT was not appropriate. We now report on commissioning and pre-clinical dosimetric evaluation of an upcoming novel Monte Carlo (MC) calculation algorithm for robotic radiosurgery with MLC.

#### Material and Methods

For commissioning of the MC algorithm, source parameters were iteratively adjusted to match water tank measurement data acquired with unshielded diodes. Dosimetric verification was performed with radiochromic film (EBT 3) in a phantom with slabs of different density. The phantom consisted of two 3.5 cm thick layers of solid water ( $\alpha=1$  g/cc) enclosing one layer (6.7cm) of lung-equivalent balsa wood ( $\alpha=0.1...0.3$  g/cc). The film was positioned perpendicular to the slabs in crossplane orientation. Quadratic fields of different size (23.0 x 23.1 mm<sup>2</sup> to 100.0 x 100.1 mm<sup>2</sup>) were delivered to the phantom, with the film plane parallel the beam central axis. FSPB and MC calculated dose distributions were compared to film measurements using FilmQA (3cognition, Inc.). For single beams, gamma criteria of 5%/1 mm and 3%/1 mm (global gamma, limited to ROIs enclosing 1.5 times the beam size) were selected. For detailed local characterization, line scans were evaluated using ImageJ v1.51j (Rasband, W.S., U.S. National Institutes of Health, USA).

#### Results

For beam commissioning, best correspondence between MC-calculated dose to water and diode measurements was achieved with a max beam energy setting of 6.3 MeV, a Gaussian source distribution with 1.8 mm FWHM and default settings for MLC transmission modelling. Film measurements in the variable density slab phantom corresponded much better with MC compared to FSPB calculations, with higher gamma pass rates of 95.4 +/- 1.2 % vs. 62.2 +/- 5.9 % (5%/1 mm) and 82.0 +/- 2.6 % vs 48.8 +/- 8.0 % (3%/1 mm). Contrary to FSPB, MC correctly predicts a decrease in dose upon entering low density tissue. Yet, non-negligible discrepancies at the transition from very low density material (<0.15 g/cc) to higher density material were identified, presumably due to different assumptions in the MC algorithm for particle transport below and above this density threshold, which affected calculated dose to film.

#### Conclusion

The novel MC dose algorithm improves calculation accuracy in heterogeneous tissue, potentially expanding the clinical use of robotic radiosurgery with MLC.

**EP-1812 Proton pencil beam scanning with motion emulated as spot shifts: dose reconstruction for lung cancer**

S. Damkjær<sup>1</sup>, L. Hoffmann<sup>2</sup>, D.S. Møller<sup>2</sup>, J.B.B. Petersen<sup>2</sup>, M. Josipovic<sup>1</sup>, G.F. Persson<sup>1</sup>, P. Munck af

Rosenschöld<sup>3</sup>, P.R. Poulsen<sup>2</sup>

<sup>1</sup>Rigshospitalet Copenhagen University Hospital, Department of Oncology, Copenhagen, Denmark

<sup>2</sup>Aarhus University Hospital, Department of Oncology, Aarhus, Denmark

<sup>3</sup>Skåne University Hospital, Radiation Physics, Malmö, Sweden

#### Purpose or Objective

Proton pencil beam scanning (PBS) may improve radiotherapy of lung cancer, but respiratory motion causes uncertainties in the delivered dose. The impact of the motion can be estimated by splitting the treatment plan into phase specific plans that are calculated in separate 4DCT phases and summed in a reference phase by deformable image registration (DIR). This approach is, however, labor intensive, difficult to automate, highly susceptible to DIR errors and limited to the 4DCT motion. We investigated use of simple spot shifts (SS) as an alternative method to estimate the dosimetric impact of target motion. The SS method is fast, straightforward to automate, easier to interpret and applicable to any motion observed during treatment.

#### Material and Methods

The SS method emulates beam's-eye-view target motion as proton spot shifts and in-depth motion as energy changes and performs all dose calculation in the exhale 4DCT phase. The method was tested for a challenging lung cancer case with two small targets (a primary 1.5 ml tumor (T) in the lower left lobe and a 4.8 ml lymph node (LN) in station 8) and large respiratory motion (T: 20mm, LN: 6mm). We simulated treatment delivery in full inhale with dose evaluation in the full exhale phase. A test plan was created with two spots hitting the center of the two targets in the inhale phase (Fig 1A+D). The dose in the exhale anatomy was estimated by warping the inhale dose to the exhale phase by DIR (Velocity) (Fig 1B+E) and by calculating the dose directly in the exhale phase by the SS method using different spot shifts for T and LN (Fig 1C+F). Next, a full single field PBS plan was calculated in the inhale phase and the dose was again estimated in the exhale phase by dose warping and SS calculation. Target doses were compared between methods.

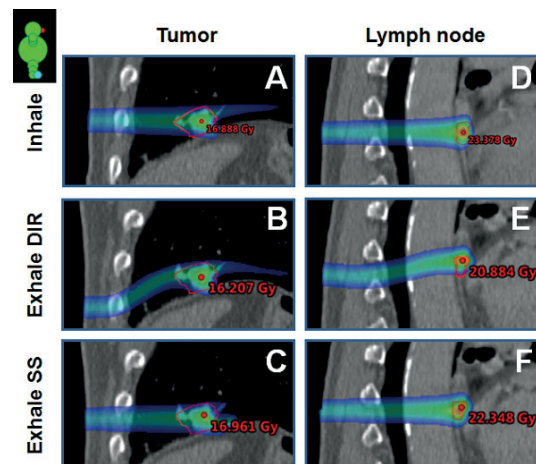


Figure 1: Dose distributions of the two-spot plan on the maximum inhale phase for the T (A) and LN (D) targets. Warped doses and doses found by the spot shift method are shown for the T (B and C) and LN (E and F), respectively.

#### Results

The DIR and thus dose warping highly depended on the defined deformation volume. The warped dose in the exhale phase represented rib and tumor doses well while the entrance dose in the lung was clearly wrong due to insufficient modelling of the sliding pleura motion by the DIR (Fig 1B). Although the SS method used a wrong entrance path through the ribs the target doses agreed well with the original inhale doses (Fig 1D+F). The Dice index between warped and SS dose in the exhale phase